Pediatric Radiology (2022) 52:429–444
https://doi.org/10.1007/s00247-021-05196-4

PICTORIAL ESSAY

Pediatric chest wall masses: spectrum of benign findings on ultrasound

Philip G. Colucci[1] · Sara A. Cohen[1] · Michael Baad[1] · Christy B. Pomeranz[1] · Lee K. Collins[1] · Arzu Kovanlikaya[1]

Received: 26 April 2021 / Revised: 20 July 2021 / Accepted: 18 August 2021 / Published online: 10 September 2021

Abstract

A palpable finding along the chest wall is a frequent indication for pediatric US. Accurate identification of benign lesions can reassure families and appropriately triage children who need follow-up, cross-sectional imaging, or biopsy. In this pictorial essay, we review chest wall anatomy, illustrate US techniques and discuss key US imaging features of common benign lesions and normal variants.

Keywords Benign neoplasm · Chest · Chest wall · Children · Soft-tissue mass · Thorax · Ultrasound

Introduction

Requests for radiologic evaluation of chest wall lesions are common in the pediatric population. This region can be particularly challenging to assess, owing to unique anatomical features and disease processes found only in this region. A vast majority of these lesions are benign when painless [1], and with thorough knowledge and experience, a specific diagnosis can often be made without the need for cross-sectional imaging.

Chest wall lesions commonly present in the pediatric population, some overlapping with those found in adults and others unique to pediatrics [2]. The spectrum of abnormalities includes normal variants, superficial neoplasms, sequela of trauma, and rib and chest wall musculature abnormalities. Often referred as outpatients for a superficial skin lesion or palpable abnormality, the first-line imaging modality is typically US, radiograph or both concurrently [3–5]. Many of these lesions are radiographically occult; therefore, US is crucial in determining the diagnosis and follow-up. If further evaluation is required, the US appearance determines whether CT or MRI is most appropriate. Although some clinical questions require multiple imaging modalities, US often fully characterizes normal chest wall anatomy and diagnoses many benign processes. Differentiating benign and malignant masses on US, however, can be challenging in children. Unless a lesion is a simple cyst or lipoma, malignancy should be a consideration [6]. Sonographic criteria suggestive of malignancy in adults such as size, margins and depth often do not apply to children, in whom small, superficial, circumscribed lesions can be malignant [6, 7]. Correlation with clinical history is fundamental and findings such as pain, tenderness or interval growth can increase concern for a malignant mass [1, 8]. In addition, the presence of multiple superficial masses can raise suspicion for malignancy such as metastatic neuroblastoma or leukemia [6]. Many sonographic features of benign lesions overlap with malignancy and often histological diagnosis is necessary.

We present a consolidated sonographic review of benign chest wall masses that arise in the pediatric population. It is important for the radiologist to be familiar with these sonographic findings to improve diagnostic confidence and avoid unnecessary additional workup whenever possible.

Technical considerations

Ultrasonography is a relatively inexpensive examination that allows for static and real-time gray-scale imaging in addition to color and spectral Doppler evaluation. The ability to characterize non-ossified structures is especially important for the

CME activity This article has been selected as the CME activity for the current month. Please visit the SPR website at www.pedrad.org on the Education page and follow the instructions to complete this CME activity.

✉ Sara A. Cohen
sac7008@med.cornell.edu

[1] Department of Radiology, Weill Cornell Medicine/New York Presbyterian Hospital, 525 E. 68th St., New York, NY 10065, USA

chest wall because a significant portion of the rib cage is cartilaginous. One of the challenges with US is inter-user variability, which can be mitigated to some degree by technical experience and comprehensive clinical knowledge.

A linear, high-frequency (9–17 MHz) transducer provides excellent soft-tissue contrast and spatial resolution and should be used when interrogating superficial structures. Spatial resolution is maximal at the focal zone, so it is important to ensure the focal zone is placed at a depth near the area of interest. Imaging of superficial structures immediately subjacent to the transducer can result in degraded resolution, which can be mitigated by using a stand-off pad or extra US gel to increase the distance between the transducer and the target. Other US parameters, such as transmit gain and time gain compensation, should likewise be appropriately adjusted. Setting the gain too high can artifactually make an anechoic simple cyst appear hypoechoic, while setting the gain too low can make the features of a complex cyst difficult to appreciate.

Images should always be acquired in longitudinal and transverse planes with respect to the adjacent anatomy. For instance, a lesion overlying the sternum can be displayed in true axial and sagittal planes but a lesion overlying a rib should be imaged longitudinal and transverse to the plane of the rib, which is often oblique to the chest wall. A cinematic sweep that extends beyond a lesion in all directions should always be uploaded for radiologist review on a diagnostic workstation. The presence or absence of vascularity should always be documented with color Doppler imaging, with the color scale set at an appropriate level. If vascularity is present, then the flow should be further characterized with spectral waveforms. Representative images of the contralateral side are often helpful as a comparative reference.

The final component in achieving ideal images involves maximizing coordination and cooperation. Fortunately, the low ambient light in the examination room is calming for most children and US equipment tends to be less intimidating than other imaging modalities because the equipment is relatively small and virtually silent. All supplies should be readily available and immediately accessible, chairs and beds should be easily adjustable, and the child should be positioned in a way that prioritizes comfort while maintaining accessibility. Whenever possible, the child should be held or comforted by a caregiver throughout the US examination.

Prior to image interpretation, it is good practice for the radiologist to physically inspect the lesion for consistency, mobility, size, localized warmth, palpable thrill and associated skin changes. These physical exam findings can directly influence and narrow the differential diagnosis. The radiologist should scan the lesion whenever possible, particularly if there is a confusing or indeterminate lesion. If direct inspection is not feasible, the technologist should be asked about these findings and might provide pictures, which can be added to the electronic medical record or picture archiving and communication system (PACS). The child or guardian should also be asked about critical elements of the child's history (presence of pain, length of time, noticeable changes in size, presence of trauma, discharge) that are not available in the provided history or notes.

Normal chest wall anatomy

The pediatric chest wall encompasses relatively consistent normal anatomy (Fig. 1). The sonographic appearance can be confusing because numerous structures exist in close proximity. The skin is echogenic and should be uniform in thickness. It is seen as two parallel echogenic lines: the epidermal "entry echo" between the transducer and the skin, with the echogenic dermis beneath. Immediately subjacent to the skin is subcutaneous fat, which has a lobulated appearance with fine curvilinear hyperechoic lines caused by acoustic reflections from interdigitating fascia. This tissue is most often the reference used to describe relative echogenicity. Musculature is slightly hypoechoic and has a striated appearance. The ossified and non-ossified portions of the rib cage can be followed in entirety. The superficial cortex of ossified bone is visualized as markedly hyperechoic with complete posterior acoustic shadowing. Cartilage and non-ossified bone are homogeneously hypoechoic and allow for interrogation of subjacent anatomy. The pleura is also markedly echogenic but the subjacent air-filled lung demonstrates "dirty" shadowing, producing artifactual echoes that extend deep to the pleura and do not provide anatomical detail. Absence of this normal artifact might indicate an intrathoracic process (i.e. pleural effusion, pulmonary consolidation, etc.). Blood vessels should be nearly anechoic and can be confirmed to have flow with color, power or spectral Doppler imaging.

Congenital costochondral abnormalities

Chest wall anatomical variations are the most common pediatric anterior chest wall lesion and usually have no clinical significance [1, 9, 10]. Multiple developmental variations can result in a palpable mass, especially in the setting of asymmetry. The most common etiologies include focal convex angulation of the costal cartilage (Fig. 2), asymmetry of the costal cartilage, paracostal subcutaneous nodules, a tilted sternum, and pectus excavatum or carinatum [9, 11, 12]. Abnormal fusion of adjacent costal cartilages might also be palpable, even in the absence of outward angulation (Fig. 3). The sternalis muscle is present in approximately 8% of the population and is unilateral in approximately two-thirds of cases [13]. Costochondral subluxations from either acute trauma or connective tissue diseases, such as Ehlers–Danlos syndrome, might also be present (Fig. 4). Although this entity is

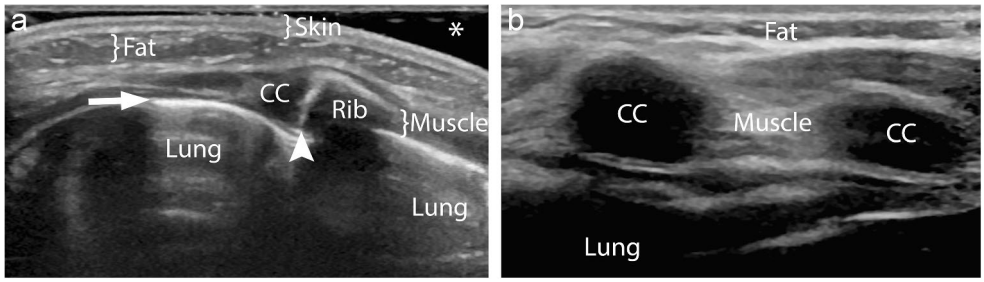

Fig. 1 Normal pediatric chest wall anatomy in an 8-year-old girl. **a, b** Gray-scale obliquely oriented images of the chest obtained longitudinal (**a**) and transverse (**b**) to the plane of the rib demonstrate structures routinely appreciated on sonography, including the skin, subcutaneous fat, musculature, bony rib, costal cartilage (*CC*), costochondral junction (*arrowhead*), pleura (*arrow*) and lung. Extra gel is used as a stand-off pad (*asterisk*)

usually treated conservatively, it can be important to identify as a child's source of pain. Much more rarely, Poland syndrome is characterized by hypoplasia or absence of soft tissues (classically the pectoralis major musculature) and sometimes presents with associated chest wall deformities [14]. Many of these findings are radiographically occult [12]. In all cases, the contralateral anatomy is a valuable reference to assess for symmetry.

Traumatic costochondral abnormalities

Although typically less sensitive for osseous pathology than other modalities, US serves an important role in a chest wall trauma workup, even in the setting of normal radiographs. In addition to cartilage and non-ossified bone being radiographically occult, nondisplaced acute fractures of ossified ribs are often not appreciable on radiographs, even with dedicated views [15]. It has been shown that US is more sensitive than radiographs for the detection of acute rib fractures in adults [15, 16] and can detect radiographically occult rib fractures and costochondral separations in children undergoing workup for nonaccidental trauma [17, 18].

For the ossified rib, hematoma or early callous formation and even cortical discontinuity can be sonographically evident (Fig. 5). Fractures involving non-ossified costal cartilage can appear as a relatively echogenic fracture line with or without step-off deformity [19, 20]. Costochondral and chondrosternal separations might be accompanied by linear gas, presumably from vacuum phenomenon, which also appears echogenic [19, 20]. Furthermore, US is a dynamic examination, and provocative maneuvers can accentuate subtle chest wall injuries. For instance, Valsalva technique might demonstrate extrusion of hemorrhagic and inflammatory debris in the setting of a fracture isolated to cartilage (Fig. 6). Although rare, lung herniation can occur with blunt force trauma [15]. Rib fractures as well as injuries to the sternum in younger children should raise suspicion for nonaccidental trauma and prompt a skeletal survey.

Osteochondroma

Osteochondroma (or exostosis) is a benign bony growth covered by a cartilage cap. The prevalence of a solitary osteochondroma in the general population is estimated to be 1–2%; it is the most common bone tumor in children, and overall accounts for up to 50% of benign bone tumors [21, 22]. These lesions usually arise at the metaphysis of long bones or along metaphyseal equivalents such as the portion of the rib near the costochondral junction. An osteochondroma typically presents as a hard, immobile, palpable mass. Pain is uncommon but if present can be caused by overlying bursitis, nerve impingement, vascular compression, pseudoaneurysm formation or possibly fracture. If there are

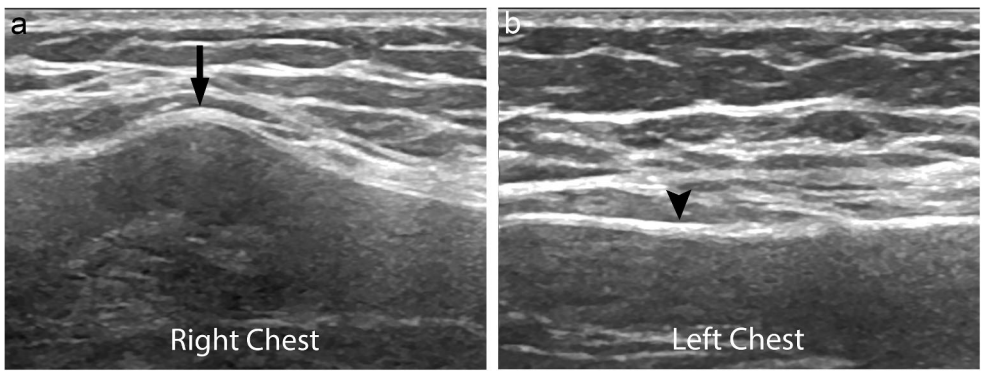

Fig. 2 Angulated costal cartilage in a 10-year-old boy presenting with a painless anterior chest bulge. **a, b** Gray-scale US longitudinal to the plane of costal cartilage (**a**) shows anterior angulation of a costal cartilage at the site of palpable concern (*arrow*) compared to the smooth surface (*arrowhead*) of the contralateral side (**b**)

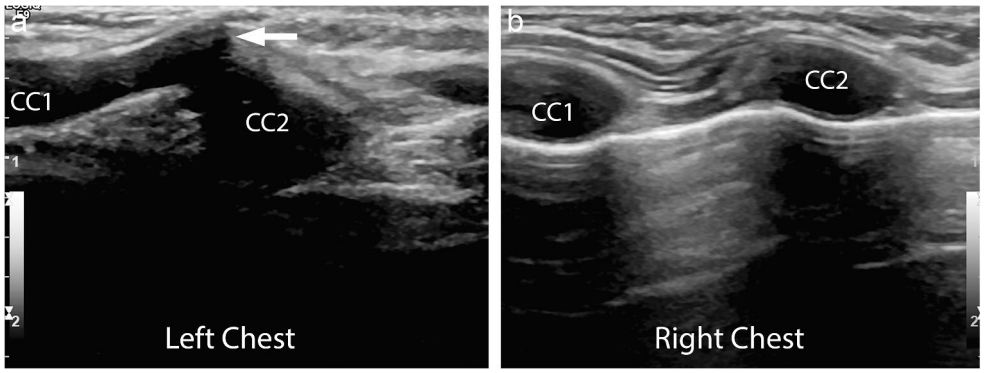

Fig. 3 Fused costal cartilages in a 2-year-old boy with palpable lump. **a** Gray-scale US transverse to the plane of the costal cartilage shows fusion of two adjacent costal cartilages (*CC1* and *CC2*) with focal anterior angulation (*arrow*). **b** Gray-scale US image transverse to the plane of the costal cartilages of the normal contralateral side shows separate costal cartilages (*CC1* and *CC2*)

multiple lesions or the osteochondroma is sessile then hereditary multiple exostoses should be considered.

A pedunculated osteochondroma arising from a rib or scapula has the sonographic appearance of an expansile bony protuberance with cortical continuity (Fig. 7). Larger lesions might be evident on radiographs or CT, but small or sessile osteochondromas are sometimes radiographically occult. The osseous component typically continues to grow until the child achieves skeletal maturity, and it can accelerate in growth during puberty. The overlying cartilage cap is well evaluated with US and often appears homogeneously hypoechoic, similar in echotexture to normal costal cartilage. If mineralization is present in the cartilage cap then it will appear echogenic with a variable amount of shadowing. Malignant transformation is rare, occurring in approximately 1% of solitary osteochondromas, and this is unusual in patients younger than 20 years [23]. Once skeletal maturity is reached, an upper limit of 2 cm has a reported sensitivity of 100%, with 95–98% specificity on CT and MR, respectively [24]. In a child, chondrosarcoma should be suspected if the cartilage cap is greater than 3 cm in thickness [23]. Osteochondromas demonstrate no abnormal vascularity on color Doppler and the surrounding structures should appear normal.

Ganglion/synovial cyst

The terms ganglion and synovial are often used interchangeably. Synovial cysts are lined with synovial cells and are thought to represent a herniation of joint fluid. Ganglion cysts are encapsulated by fibrous connective tissue instead of synovium and their pathogenesis remains unclear. They might represent an extra-synovial herniation of joint fluid or be caused by a myxoid degenerative process or repeated trauma [25]. Either type of cyst can be treated with percutaneous aspiration (often with corticosteroid injection and fenestration) or surgical resection, although recurrence is common. Addressing any internal derangement in the adjacent joint can simultaneously address the underlying cause for synovial cyst formation [26].

Ganglion and synovial cysts are indistinguishable on imaging. Both are typically well-circumscribed anechoic cysts

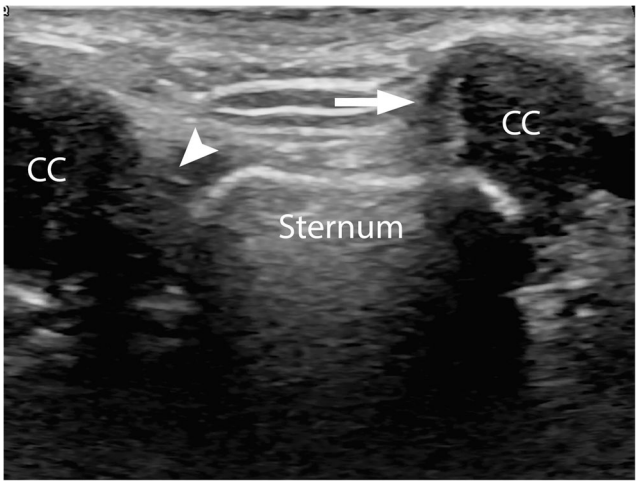

Fig. 4 Sternocostal subluxation in a 10-year-old girl presenting with chest wall protuberance. Transverse gray-scale US image shows that the left costal cartilage (*CC*) is positioned anteromedially (*arrow*) with respect to the normal right sternocostal articulation (*arrowhead*)

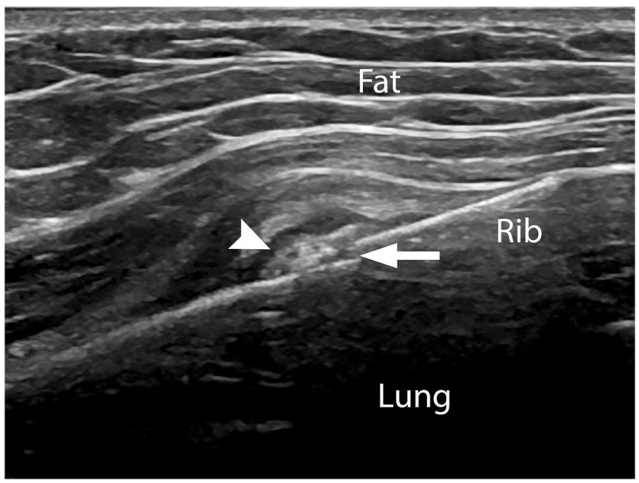

Fig. 5 Rib fracture in a 16-year-old boy following a fall 3 weeks prior. Gray-scale US longitudinal to the plane of the rib shows a rib fracture with cortical disruption (*arrow*). Within the superficial soft tissues, there are ill-defined echogenic foci (*arrowhead*), consistent with developing callus formation

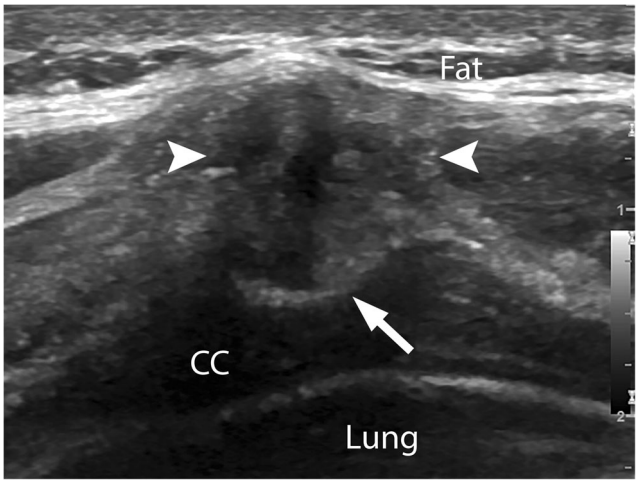

Fig. 6 Costal cartilage injury in a 14-year-old boy presenting with a palpable lesion and associated clicking sound after trauma. Gray-scale US longitudinal to the plane of the costal cartilage (*CC*) demonstrates discontinuity of the cartilaginous portion of the rib (*arrow*) with heterogeneity of the overlying deep soft tissue (*arrowheads*), likely edema and hemorrhage

with thin walls and posterior acoustic enhancement (Fig. 8). Ganglion cysts have been rarely described to have a solid appearance, possibly related to decompression prior to imaging [27]. Both can be found in juxta-articular locations, but ganglion cysts also occur in close proximity to or directly involve tendons and nerves. Both sometimes have a beak-like neck extending toward a nearby joint (Fig. 8). Evidence of possible communication with a joint should always be described because the neck must be resected in entirety to minimize the chance of recurrence after resection. These cysts have varying degrees of complexity including increased echogenicity, thick walls and multiple loculations, but there should be no evidence of internal flow on color Doppler imaging (Fig. 8). A small degree of peripheral or septal vascularity might be identified, possibly from normal synovial vasculature or inflammation from rupture.

Fat-containing lesions

A lipoma is a benign tumor composed entirely of mature fat cells. It is the most common fat-containing tumor in children and represents almost 50% of soft-tissue tumors across all ages [28]. Lipomas can be found at any location where adipose tissue normally exists, most commonly in the subcutaneous tissues. They tend to be slow growing but can accelerate with weight gain. Lipomas are usually clinically evident and correctly diagnosed, but several other fat-containing lesions can have overlapping clinical features. Lipoblastoma is the second most common fatty tumor in young children and is similar to lipoma except that it contains both mature and immature fat cells, usually occurs before the age of 3, might demonstrate more rapid growth, and is more frequently found in the extremities [29]. Lipofibromatosis is a rare lesion also seen in young children, more commonly found in the distal extremities (hands and feet). Imaging demonstrates variable amounts of fat and fibrosis, and diagnosis is only definitively made with biopsy [30]. Liposarcoma is very rare in children, with myxoid liposarcoma being the common form. Finally, angiolipoma should be considered if the mass is painful, especially in older children.

Superficial lipomas are most often isoechoic to the adjacent subcutaneous fat but demonstrate variable echogenicity and can be hyperechoic or hypoechoic (Fig. 9). The internal echotexture is also similar to the adjacent fat, often with undulating striations or linear bands. An echogenic capsule might be present. No significant acoustic enhancement or shadowing is present. A simple lipoma has no increased internal vascularity (Fig. 9). Lipomas commonly have striations and internal structure that parallel the surrounding tissue, in contradistinction to angiolipomas (a subtype of regular lipomas), which tend to be more ovoid and well circumscribed. Internal vascularity is also reported in 23% of angiolipomas [31], further helping to distinguish these from a standard lipoma [31]. Angiolipomas also tend to be smaller than regular lipomas, <2 cm, and demonstrate pain on palpation, which diminishes over time [31]. In general, any lipoma demonstrating internal vascularity or reported to be painful should undergo histological sampling.

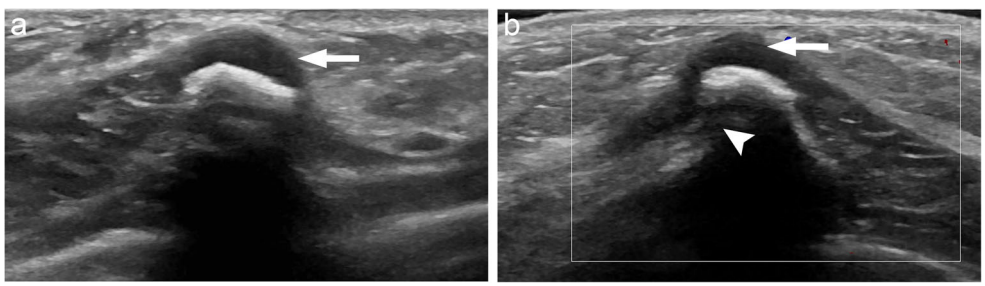

Fig. 7 Osteochondroma in a 4-year-old girl presenting with palpable rib lump. **a, b** With respect to the plane of the rib, longitudinal gray-scale (**a**) and transverse color Doppler (**b**) US images show a bony protuberance arising from the rib with cortical continuity (*arrowhead*), hypoechoic cartilage cap (*arrow*) and minimal vascularity

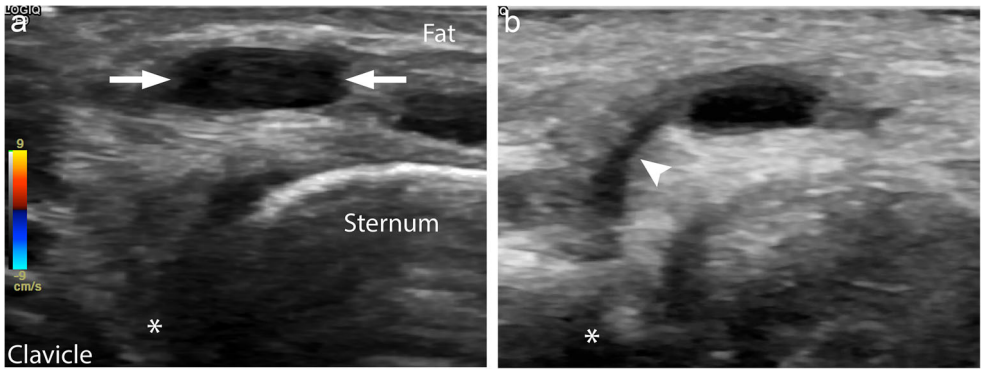

Fig. 8 Ganglion/synovial cyst in a 6-year-old boy presenting with a lump at the left sternoclavicular junction. **a, b** Transverse color Doppler (**a**) and gray-scale oblique (**b**) US images show an anechoic avascular cystic lesion (*arrows*) overlying the sternoclavicular joint (*asterisk*) with beak-like neck extending toward the joint (*arrowhead*)

Accessory breast tissue

Accessory breast tissue is seen in up to 6% of the population [32]. The axilla is the most common location, with additional sites usually along the milk line, which extends from the anterior axillary fold to the medial inguinal fold, though accessory breast tissue has been reported throughout the trunk, face and proximal extremities. Accessory breast tissue is usually asymptomatic. In the absence of an associated supernumerary nipple, the initial presentation is likely to occur during times where normal breast tissue is subject to hormonal stimulation such as thelarche (the onset of pubertal breast development), menarche, pregnancy or lactation. The pediatric patient might experience periodic pain or swelling in the ectopic location during puberty. Nipple discharge is rare in children and adolescents but theoretically could occur in the setting of a supernumerary nipple. The sonographic appearance of accessory breast tissue is identical to that of normal fibroglandular tissue (Fig. 10). Malignancy is rare, but it is important to remember that all breast pathology, benign and malignant, can occur in accessory breast tissue [33, 34].

Gynecomastia

Gynecomastia is the development of glandular breast tissue in a male, which can occur unilaterally or bilaterally. Physiological gynecomastia most commonly occurs in the neonate, adolescent and adult older than 50. Maternal hormones pass freely into the fetal circulation and a palpable subareolar mass can be observed in up to 90% of male neonates [35] (Fig. 11). This is a self-limited process that typically resolves in the first few weeks after birth. During adolescence, gynecomastia has been reported to occur in up to 60–75% of normal healthy boys [36]. The child might present with a discrete palpable mass or more diffuse breast enlargement, often with associated pain or tenderness. This is also a self-limited process. Multiple non-physiological causes of gynecomastia present at any age and include neoplasm, systemic dysfunction, genetic anomalies and medication-induced. Regardless of the etiology, the sonographic appearance of gynecomastia can be classified as nodular, dendritic and diffuse [37]. Nodular gynecomastia tends to be a well-defined, hypoechoic mass with variable amounts of ductal development, which appear as anechoic tubular structures (Fig. 12). The dendritic pattern is also hypoechoic but more flame-shaped with irregular borders (Fig. 13). Diffuse gynecomastia generally has the appearance of normal fibroglandular tissue. These lesions often appear avascular, though a minimal amount of internal vascularity is entirely normal.

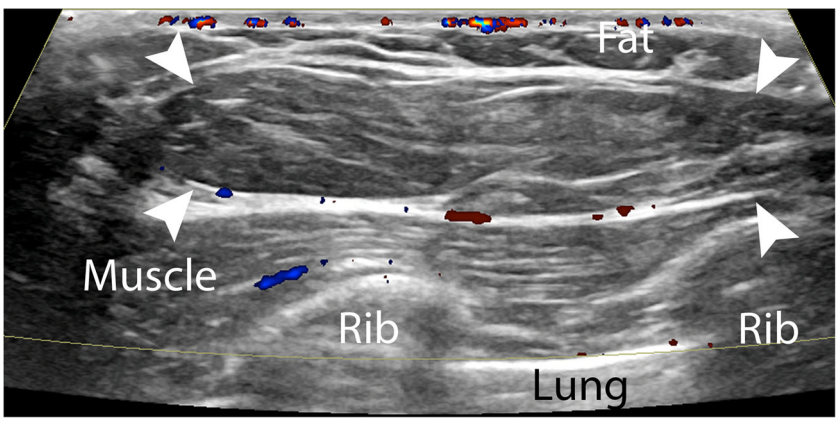

Fig. 9 Lipoma in a 17-year-old girl presenting with a chest wall mass. Longitudinal color Doppler US image shows a well-circumscribed isoechoic oblong lesion (*arrowheads*) with echotexture similar to adjacent subcutaneous fat. There is an echogenic capsule, echogenic curvilinear striations parallel to the skin surface, and no significant vascularity

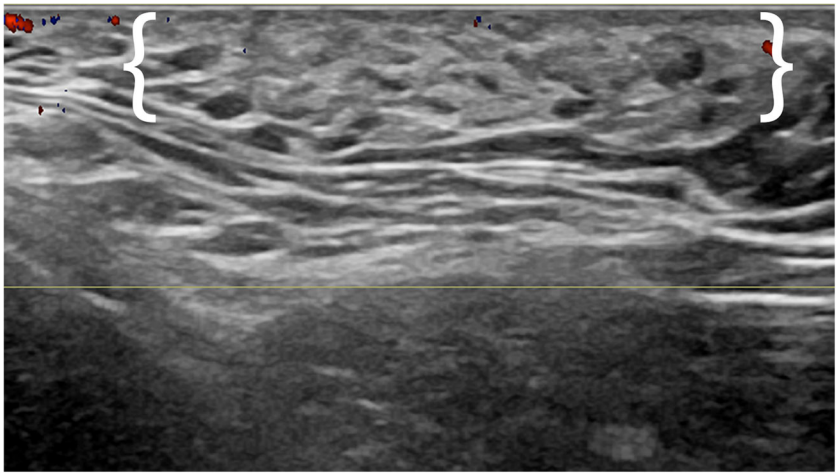

Fig. 10 Accessory breast tissue in a 17-year-old girl presenting with palpable mass in the right axilla with pain and burning. Longitudinal color Doppler US image shows an axillary mass of fibroglandular breast tissue (*brackets*)

Mammary duct ectasia

Mammary duct ectasia is the most common cause of bloody nipple discharge in childhood and presents as a periareolar palpable mass or breast enlargement [38]. This is a benign condition characterized by dilated mammary ducts with periductal inflammation and fibrosis [38, 39]. The cause is unknown and proposed etiologies include bacterial infection, hormonal factors and developmental abnormality [38]. Mammary duct ectasia is more common in girls, has been reported in infants as young as 2 months, and can be unilateral or bilateral [38]. The condition is usually self-limited, with spontaneous resolution. Sonographic findings include dilated anechoic tubular lesions or cysts, which might be simple or complex [33, 38] (Fig. 14). Echogenic debris might be present, suggesting hemorrhage [38].

Abscess/purulent soft-tissue infection

In the setting of a soft-tissue infection, US can help differentiate between nonpurulent cellulitis and purulent processes with and without a drainable collection. This distinction helps guide treatment because children with a collection might benefit from incision and drainage [40–42]. Soft-tissue infection has been observed to progress in a step-wise fashion starting with soft-tissue thickening, proceeding to phlegmon/inflammatory mass, and eventually organizing into an abscess [43]. The size of the fluid collection might be used to help determine whether incision and drainage is warranted. Although guidelines are institution-specific, collections greater than 1–2 cm are typically candidates for drainage. In the setting of methicillin-resistant *S. aureus* (MRSA) infection, purulent collections might not demonstrate discrete well-defined walls on US; however, these might still produce drainable fluid and positive cultures [44]. Purulent MRSA infections can present with sonographic findings of cobblestoning or branching interstitial

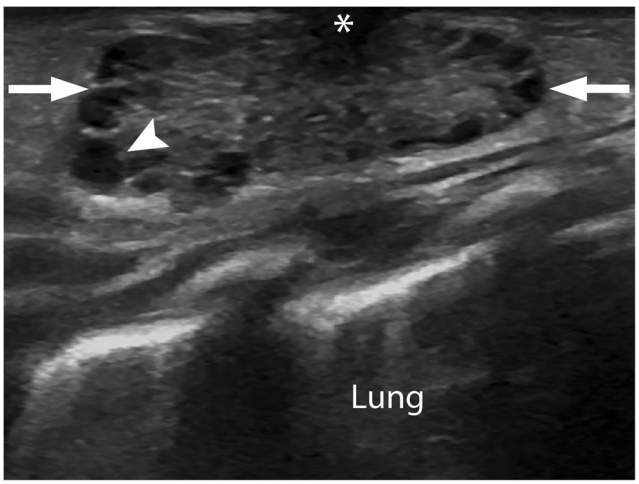

Fig. 11 Physiological enlargement of the breast bud in a 14-day-old boy. Transverse gray-scale US image shows a well-defined lesion (*arrows*) deep to the nipple (*asterisk*) with multiple prominent mammary ducts (*arrowhead*)

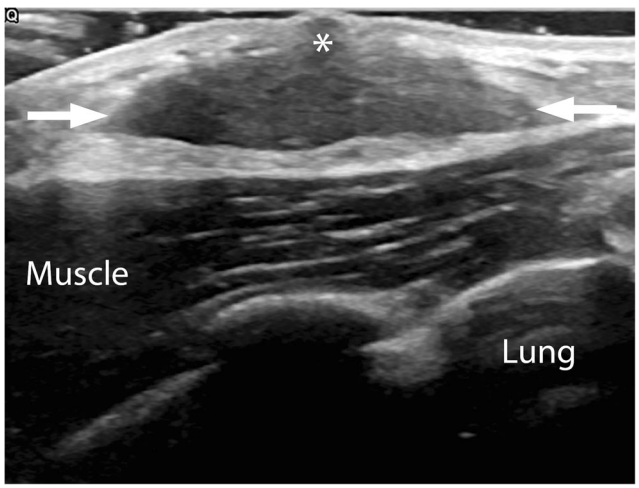

Fig. 12 Nodular gynecomastia in a 5-year-old boy presenting with a palpable lump. Transverse gray-scale US image shows a well-defined hypoechoic lesion (*arrows*) deep to the nipple (*asterisk*), consistent with nodular gynecomastia

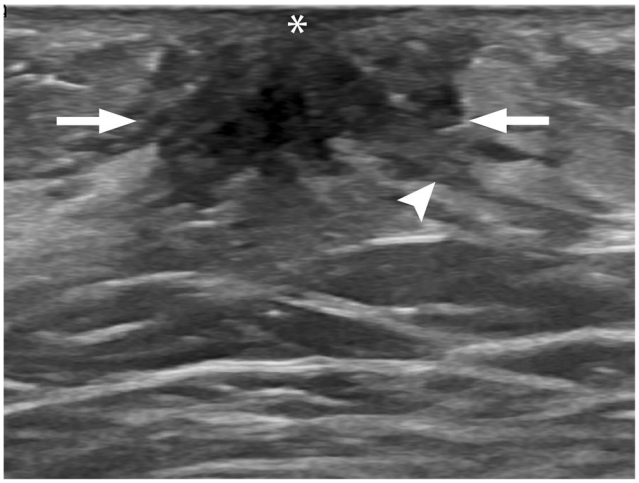

Fig. 13 Dendritic gynecomastia in a 10-year-old boy presenting with a palpable lump. Transverse gray-scale US image shows an ill-defined, flame-shape hypoechoic lesion (*arrows*) deep to the nipple (*asterisk*), with hypoechoic fingerlike projections (*arrowhead*) extending into the surrounding tissue, consistent with dendritic gynecomastia

fluid, which can overlap with the imaging appearance of cellulitis [44]. In this setting, correlation with physical exam findings of fluctuance or induration can increase suspicion for drainable purulent fluid [44]. In addition to the primary site of infection, draining lymph nodes can become enlarged from reactive hyperplasia or become necrotic and an additional nidus of infection. Finally, US might also help exclude signs of severe complications requiring urgent attention including necrotizing fasciitis, osteomyelitis and septic arthritis [45, 46]. Findings raising concern for necrotizing fasciitis include perifascial fluid, air within the deep soft tissue, and irregular or distorted appearance of the deep fascia [47].

Discrete purulent fluid collections are variable in appearance. They might be nearly anechoic or heterogeneously hypoechoic with multiple low-level echoes from the presence

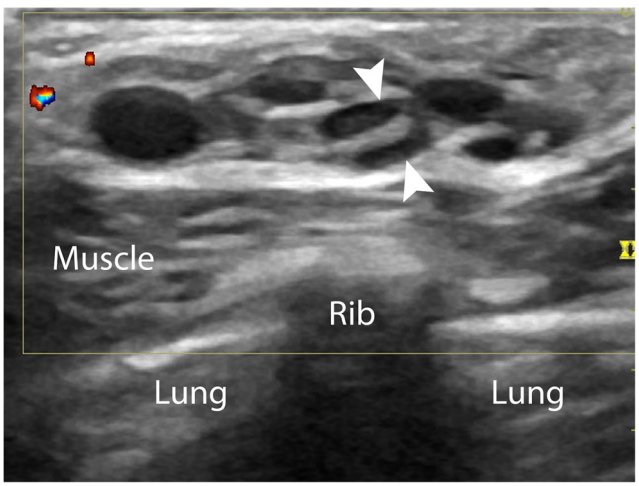

Fig. 14 Mammary duct ectasia in a 2-year-old boy presenting with bloody nipple discharge and palpable subareolar lump. Transverse color Doppler US of the retroareolar region shows multiple tubular anechoic cystic lesions (*arrowheads*) in the subcutaneous tissues without flow

of pus and other cellular debris (Fig. 15). Compression with cinematic imaging might induce movement or swirling of abscess contents, which can be especially helpful in cases where the fluid collection is nearly isoechoic to surrounding fat. An abscess will demonstrate posterior acoustic enhancement. Abscess walls tend to be thick, irregular and echogenic, though they might be less well formed in the setting of MRSA infection [44]. The surrounding subcutaneous fat is often markedly echogenic from edema. Hyperemia is evidenced by increased flow on color Doppler and is commonly seen along the abscess wall and adjacent soft tissues. Color flow should not be present within the collection, except for within thick septations if the lesion is multiloculated. The underlying bones should be closely scrutinized for evidence of subperiosteal fluid collections and frank cortical destruction (Fig. 16). Subcutaneous emphysema, from a laceration or skin defect, appears as scattered "dirty shadowing" from gas in the subcutaneous tissues. A strongly echogenic focus within the collection should raise suspicion for a retained foreign body. While metallic foreign bodies are easily seen on radiographs, US has a high sensitivity and specificity for radiolucent foreign bodies [48].

Self-limiting sternal tumors of childhood

Self-limiting sternal tumors of childhood are rare benign rapidly growing parasternal tumors arising from an exaggerated immune response to an aseptic inflammatory process [49]. These tumors typically present in infancy or young childhood, at 7–50 months of age, and rapidly grow over a period of 2 weeks [50]. These children might present with local pain and elevated body temperature. Laboratory evaluation can show mild elevation of C-reactive protein and erythrocyte sedimentation rate [49, 50]. On physical exam, the mass might feel elastic and skin can sometimes have a reddish or bluish discoloration [49]. Characteristic sonographic features in combination with young age, sternum-related location and clinical presentation can favor this diagnosis and avoid biopsy [49, 50]. On US, self-limiting sternal tumors of childhood appear as a smoothly marginated hypoechoic dumbbell-shape mass without significant internal vascularity and without invasion of surrounding structures [49–51]. The dumbbell shape occurs because the mass typically protrudes anterior and posterior to the sternum, involving the cartilage between sternal segments or between a sternal segment and cartilaginous rib [50, 51]. This often leads to an increased distance between sternal ossification centers. The diagnosis is confirmed by observation, with the lesion decreasing in size and resolving, usually within 6 months; however, this can take more than a year [50, 51]. Follow-up with US is recommended [49, 51].

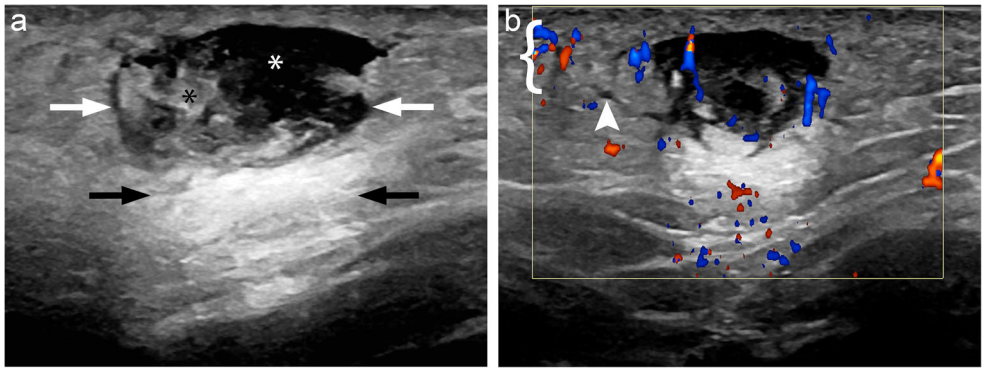

Fig. 15 Subcutaneous abscess in a 13-year-old girl presenting with enlarging chest wall "pimple." **a** Transverse gray-scale US images show an irregular cystic lesion (*white arrows*) with posterior acoustic enhancement (*black arrows*) and both anechoic (*white asterisk*) and debris-filled (*black asterisk*) portions. **b** Sagittal color Doppler US image shows predominantly peripheral vascularity. There is thickening, architectural distortion and relative hyperechogenicity (*bracket*) of the surrounding subcutaneous fat, with areas of interstitial fluid (*arrowhead*), consistent with inflammation

Myofibroma/myofibromatosis

First described in 1951 and coined "infantile myofibromatosis" by Enzinger and Chung in 1981, the 2013 World Health Organization (WHO) classification now includes myofibroma and myofibromatosis as morphological points along the spectrum of myopericytic neoplasms [52]. Up to 88% of cases arise in children younger than 2 years, but it has been recognized that myofibromas can occur in older children and adults [30, 53]. Myofibroma refers to a single lesion, usually involving the dermis or subcutaneous tissues, and often presents as a firm, flesh-colored or purple nodule. Myofibromatosis refers to multiple lesions. The most common form is solitary myofibroma, which is a single lesion only involving the skin and soft tissues; this form accounts for 50–80% of all cases and does not require any intra-abdominal or visceral imaging. In multicentric myofibromatosis, multiple myofibromas are seen involving the skin, soft tissues and deeper musculature and bones. In a third of cases of multicentric myofibromatosis, there might be visceral involvement of the solid organs. Therefore in cases of multicentric myofibromatosis, it is recommended to undergo cross-sectional imaging to screen for visceral involvement. Visceral involvement is most commonly identified in the young infant and indicates a very poor prognosis, with a 75% mortality rate, especially when the heart or bowel is affected. In cases of solitary myofibromatosis and multicentric myofibromatosis without visceral involvement, there is a high rate of spontaneous regression of myofibromas [54].

A myofibroma appears as a well-defined heterogeneous mass with posterior acoustic enhancement (Fig. 17). There might be central necrosis, which appears hypoechoic. Calcifications might be present and appear as echogenic foci with or without evidence of acoustic shadowing. Typically, no internal vascularity is identified on color Doppler but peripheral vascularity has been reported [55]. These sonographic findings are nonspecific and, in the absence of a family history, biopsy is usually warranted [56]. Differential diagnosis for this lesion includes hemangiomas, fibrous hamartoma of infancy, infantile fibrosarcoma, soft-tissue sarcoma, neuroblastoma, neurofibromas and histiocytosis [54].

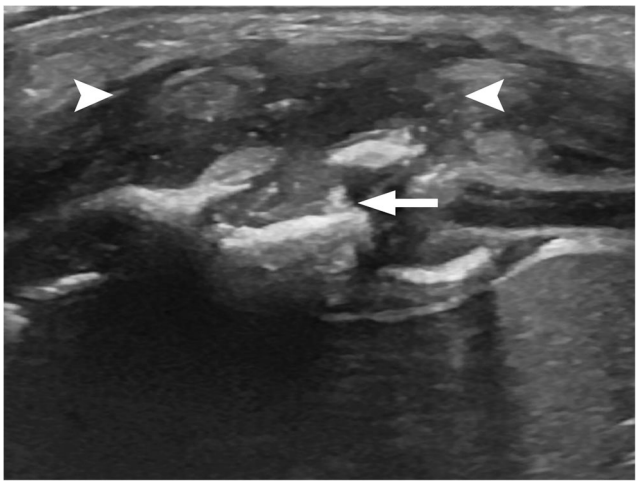

Fig. 16 Osteomyelitis of the rib in a 5-week-old girl presenting with chest wall swelling and redness. Oblique gray-scale US image shows frank cortical disruption and fragmentation of the underlying rib (*arrow*) and an adjacent hypoechoic, subcutaneous fluid collection (*arrowheads*)

Fibrous hamartoma of infancy

Fibrous hamartoma of infancy is a rare benign fibrous tumor that almost always occurs before the age of 2 years but does present as late as middle age [57]. This is generally a slow-growing tumor, though rapid growth can occur up to about age 5 years [58]. This lesion is most commonly found in the trunk, especially in the region of the axilla and shoulder [59]. Fibrous hamartoma of infancy arises in the subcutaneous tissues but can invade more deeply through fascia. If a lesion is seen primarily within the muscle, then lipofibromatosis

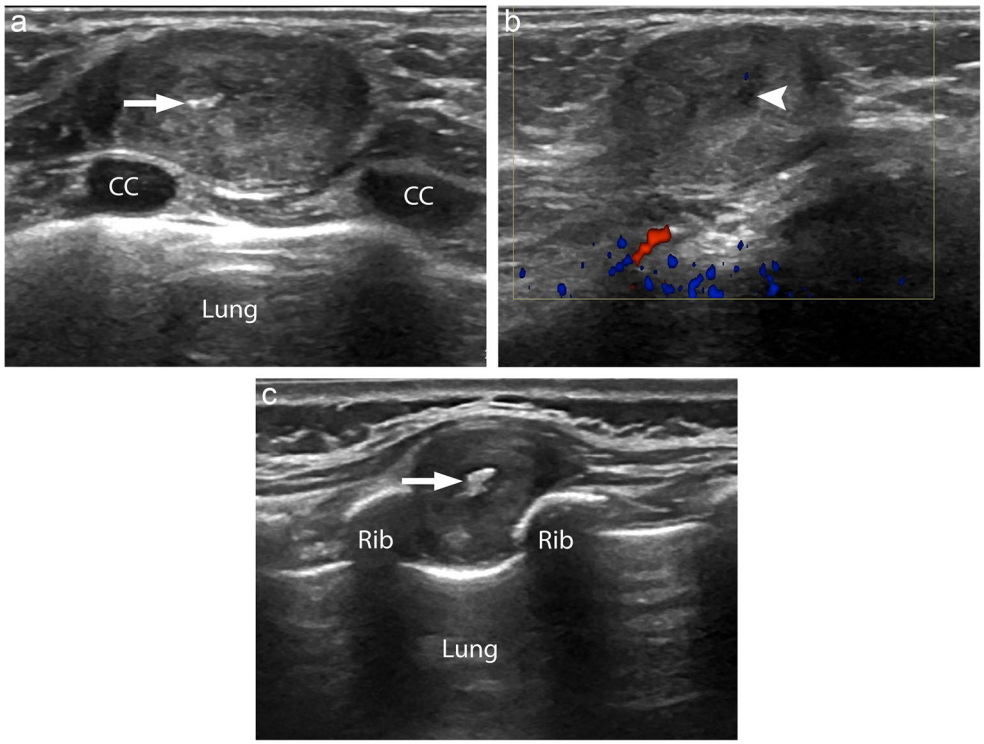

Fig. 17 Infantile myofibromas in two brothers. **a, b** Infantile myofibroma in a 6-month-old boy presenting with a palpable chest wall mass increasing in size. Longitudinal gray-scale (**a**) and color Doppler (**b**) US images show a well-defined heterogeneous mass within the subcutaneous tissue superficial to the costal cartilage (*CC*). Calcification (*arrow*) and central necrosis (*arrowhead*) are noted with minimal internal vascularity. **c** Myofibroma in the sibling, who presented at 8 weeks old with enlarging palpable chest and back lesions. Gray-scale US image shows a similar-appearing mass in the chest wall with a central calcification (*arrow*)

(previously infantile fibromatosis) or infantile fibrosarcoma should be considered [58]. Local excision is usually curative, with low recurrence rates even with incomplete excision [60]. Although recurrence rates are as high as 16%, the recurrence is usually cured by re-excision [58].

The sonographic appearance of fibrous hamartoma of infancy is nonspecific; imaging findings include an ill-defined, heterogeneously hyperechoic lesion that sometimes has a serpentine pattern (Fig. 18). As mentioned, this lesion can be locally aggressive, with involvement of the skin and extension through the fascia into the subjacent muscle. Although these features can have a worrisome appearance, this benign lesion demonstrates no significant vascularity.

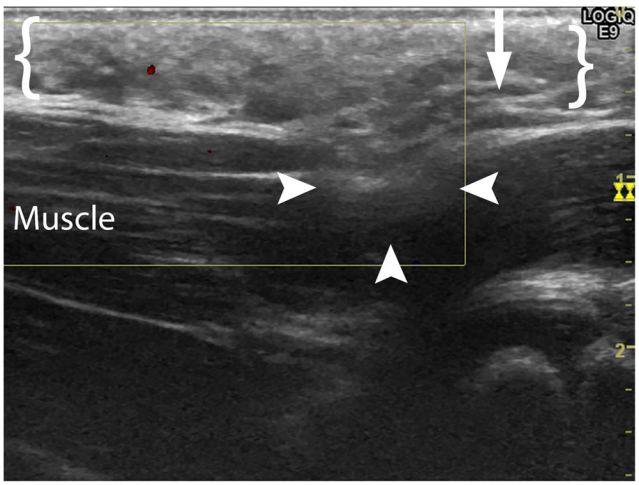

Fig. 18 Infantile fibrous hamartoma in a 1-year-old girl with nontender axillary lumps. Longitudinal color Doppler US image shows an ill-defined heterogeneously hyperechoic subcutaneous lesion (*brackets*) with a serpentine pattern (*arrow*). There is focal extension into the subjacent musculature (*arrowheads*) and no significant vascularity

Infantile hemangioma and other vascular tumors

Infantile hemangiomas present shortly after birth and progress through three phases: proliferation, plateau and involution. The lesions usually reach maximal size when the child is 3–5 months of age [61]. The involuting phase usually begins at about 12 months but might not be fully complete until 12 years of age [61]. They are most commonly found in the head and neck, with approximately 25% occurring on the trunk [61]. The classic appearance of a cherry-red or strawberry lesion infantile hemangioma might be evident on physical examination. However, if the lesion is in the deep dermis or subcutaneous tissues it can have a blueish hue (Fig. 19). In these cases, US is helpful for establishing a diagnosis so the child can receive the appropriate treatment. Screening US of the liver should be performed to exclude visceral involvement if there are five or more cutaneous infantile hemangiomas [62, 63].

The proliferating infantile hemangioma is usually a fairly well-circumscribed heterogeneous mass with variable echogenicity (Fig. 19). Color Doppler shows marked internal vascularity with

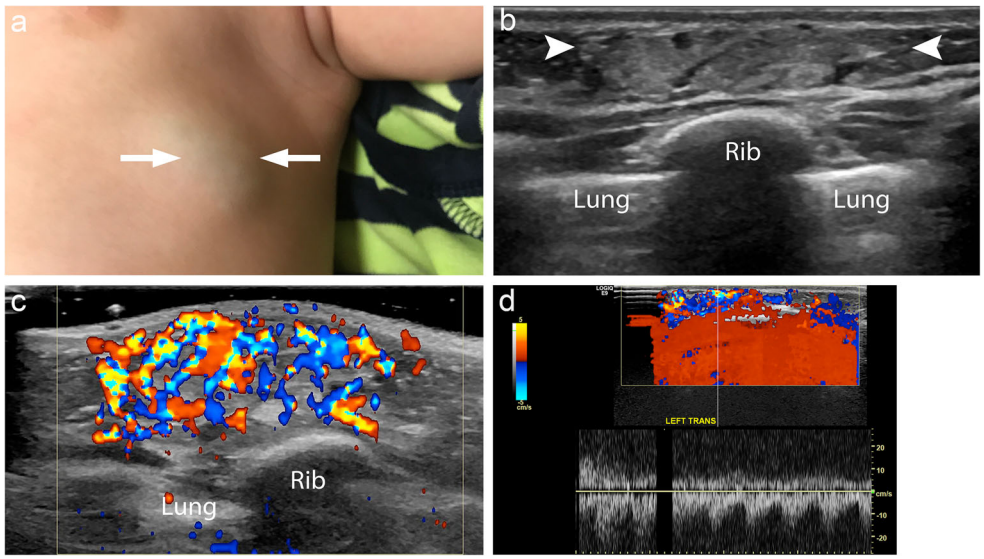

Fig. 19 Infantile hemangioma in a 6-month-old boy presenting with a chest wall mass that appeared after birth and enlarged in size. **a** Clinical photograph shows a bluish chest wall mass (*arrows*). **b** Longitudinal gray-scale US image shows a well-defined echogenic mass (*arrowheads*). **c** Color Doppler US image shows dense vascularity, more than 5 vessels/cm^2. **d** Duplex Doppler US image shows low-resistance arterial and venous waveforms

>5 vessels per square centimeter. Spectral Doppler demonstrates both venous and low-resistance arterial waveforms. During the involuting phase, there might be increased echogenicity, decreased vascularity, and increased vascular resistance [62].

Tufted angiomas are another vascular neoplasm, arising from capillary vessels, that demonstrate more aggressive behavior and imaging characteristics than hemangiomas and are closely related to Kaposiform hemangioendothelioma (Fig. 20). The tufted angioma can be distinguished from the infantile hemangioma because it can be seen at birth, is multicompartmental, and is a relatively superficial lesion, just below the skin. It might sweat more and develop relatively more hair than the surrounding skin. It can be associated with a serious complication called Kasabach–Merritt phenomenon, which is a rapid growth of the lesion resulting in thrombocytopenia, microangiopathic hemolytic anemia and consumptive coagulopathy. Kaposiform hemangioendothelioma is sometimes indistinguishable from tufted angioma on imaging and can be included in the differential diagnosis.

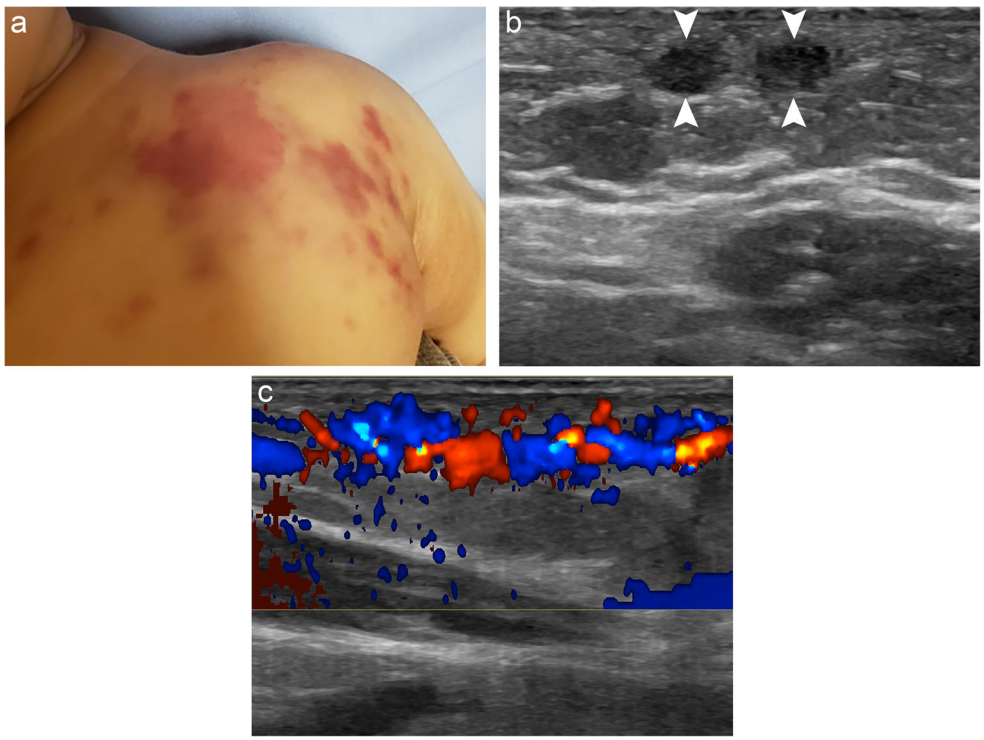

Fig. 20 Tufted angioma in a 20-week-old boy. **a** Clinical photograph shows patchy red/purple plaques on the chest wall. **b, c** Sagittal gray-scale (**b**) and color Doppler (**c**) US images show patchy ill-defined hypoechoic lesions (*arrowheads*) in the subcutaneous tissues with marked internal color flow

Vascular malformations

Vascular malformations are congenital lesions that are often present at birth but might not be noticed until childhood or later because they grow in proportion or faster than the child [64]. Growth can be exacerbated in the setting of hormonal changes, thrombosis, infection or trauma [64]. Vascular malformations can be classified as simple, which can be high flow (arteriovenous malformation, arteriovenous fistula), low flow (venous, lymphatic or capillary) or combined. US is often the first imaging test ordered in the workup of a suspected vascular malformation.

Venous malformations are the most common type of vascular malformation, and 20% of cases occur on the trunk [64]. Venous malformations have variable appearances on US, including a lobulated well-defined spongelike structure with variable echogenicity or a tortuous collection of veins [65]. Identification of only low-velocity monophasic venous waveforms on spectral Doppler can help suggest this diagnosis. If phleboliths can be identified as echogenic foci with posterior acoustic shadowing, they are pathognomonic [66]. Venous malformations are also compressible and increase in size with Valsalva [65].

Lymphatic malformations are the second most common type of vascular malformation, with 20% occurring in the axillary region [64]. Lymphatic malformations can be microcystic, macrocystic or mixed. The most recent classification system defined macrocysts as measuring more than 1–2 cm [62]. Because macrocystic lesions can be treated with percutaneous sclerotherapy, some institutions describe lesions greater than 3–4 mm as macrocystic if they are capable of being accessed [61, 67]. An uncomplicated macrocystic lymphatic malformation is typically a lobulated, nearly anechoic cystic mass with thin septations (Fig. 21). These lesions are not limited by fascial boundaries and are often transspatial. It is important to exclude the presence of intrathoracic extension, and MRI can be helpful. Few internal echoes might be evident from cellular debris. Fluid-fluid levels can be seen in the setting of intralesional hemorrhage. Internal echoes with or without fluid levels might represent infection, especially if there is surrounding hyperemia and edema. Color Doppler might demonstrate normal flow within thin septations. If intralesional flow is identified within the cystic cavities, then a venolymphatic or another slow-flow vascular lesion should be considered. Lymphatic malformations should not change in appearance with respiration or repositioning and should not collapse under pressure. These provocative maneuvers suggest a vascular component to the lesion.

Plexiform neurofibroma

Plexiform neurofibromas often involve multiple nerve segments next to the vertebral column and are considered pathognomonic for neurofibromatosis-1 (NF-1). Both the localized and diffuse forms of neurofibroma are much more commonly sporadic (approximately 10% are associated with NF-1) [68–70]. Except for the plexiform neurofibroma, which usually begins to develop in childhood, other benign nerve sheath tumors typically do not present until early adulthood.

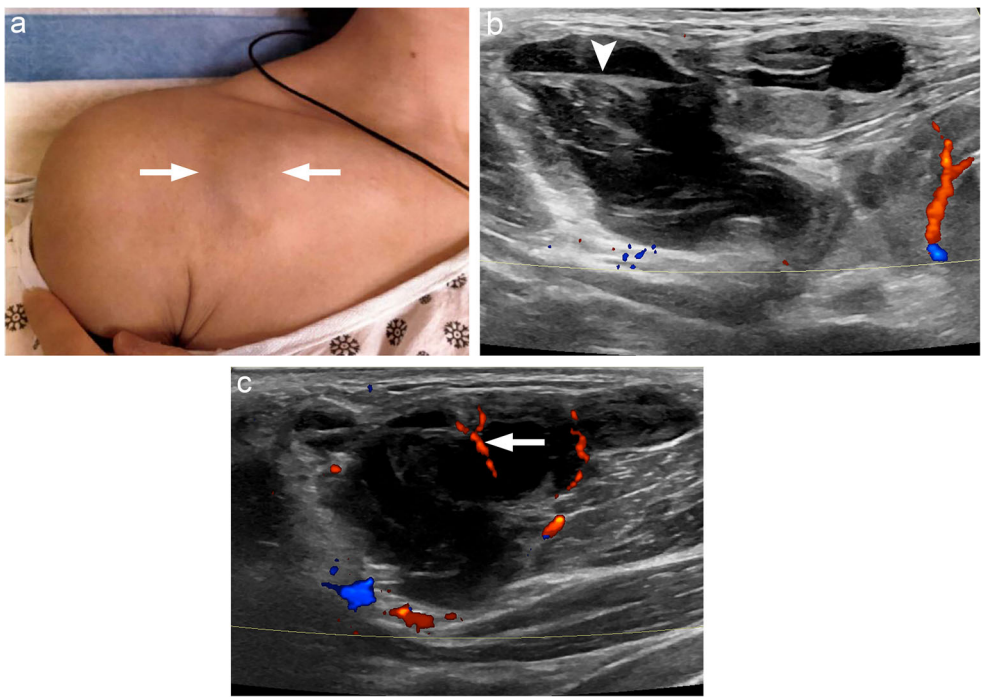

Fig. 21 Lymphatic malformation in a 16-year-old girl presenting with a painful palpable lesion for 1 week and history of a childhood cyst in the same location, which resolved. **a** Clinical photograph shows the mass inferior to the right clavicle (*arrows*). **b, c** Longitudinal (**b**) and transverse (**c**) color Doppler US images show a lobulated multiseptated mass with fluid-debris levels (*arrowhead*). Vascularity is observed along the periphery and within septations (*arrow*)

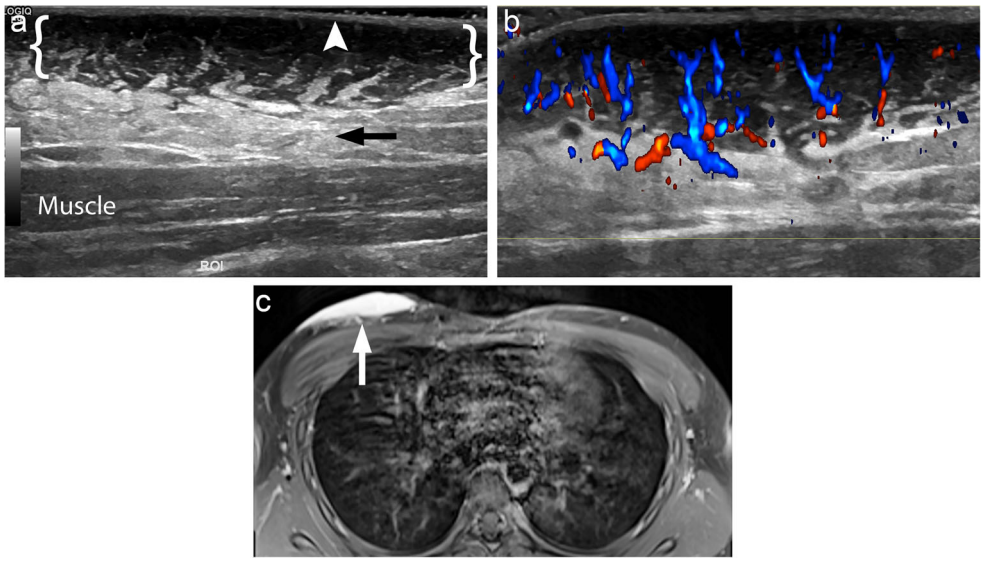

Fig. 22 Superficial plexiform neurofibroma in a 17-year-old boy with enlarging right chest wall mass. **a** Transverse gray-scale US image shows an infiltrative hypoechoic subcutaneous mass (*brackets*) with marked thinning of the overlying dermis (*arrowhead*) and diffusely increased echogenicity of the adjacent subcutaneous fat (*arrow*). **b** Transverse color Doppler US image reveals marked internal vascularity. **c** Corresponding axial T1-W fat-saturated post-gadolinium MR image shows the corresponding avidly enhancing mass (*arrow*)

Although plexiform neurofibroma is a benign lesion, it is a known precursor for malignant peripheral nerve sheath tumor, with a rate of transformation as high as 2–5% [71].

Neurofibromas are generally hypoechoic, similar to schwannomas and traumatic neuromas. The appearance of multiple adjacent enlarged nerves has often been described as a "bag of worms." Plexiform neurofibromas grow progressively and can extend beyond the perineurium (the outer-most layer of the nerve) with an aggressive, ill-defined, infiltrative and lobulated appearance (Fig. 22). The adjacent fat might be hyperechoic from regional edema, and the overlying skin might be markedly thin (Fig. 22). Color Doppler US usually demonstrates significant internal vascularity. The differential diagnosis includes vascular anomalies, soft-tissue sarcoma, and malignant peripheral nerve sheath tumors.

Dermal and epidermal inclusion cysts

Epidermal inclusion cysts (epidermoid cysts) are lined with epithelium and contain desquamated keratinized debris. Dermal inclusion cysts (dermoid cysts) are also lined with epithelium but additionally contain dermal structures such as hair follicles or glandular elements. These subcutaneous inclusion cysts, although similarly named, are unrelated to neoplastic benign cystic teratomas (e.g., ovary, mediastinum) [72, 73]. Dermal and epidermal inclusion cysts are usually asymptomatic unless they become superinfected or rupture and cause a chemical inflammatory response. Congenital dermal inclusion cysts are usually midline in location, with up to 14% occurring in the neck, sometimes in a suprasternal location [4]. Most of the radiology literature has focused on the imaging appearances of these lesions in the head and neck [72, 74]. Inclusion cysts found at other locations are often diagnosed and treated with resection, without the need for imaging [75].

Dermal and epidermal inclusion cysts cannot reliably be distinguished on US. Both are well-circumscribed, hypoechoic and often demonstrate posterior acoustic enhancement (Fig. 23). If present, echogenic debris (from calcification, fat, mucoid or purulent material) can diminish posterior acoustic enhancement or rarely even result in shadowing. Both types of inclusion cysts sometimes have an identifiable

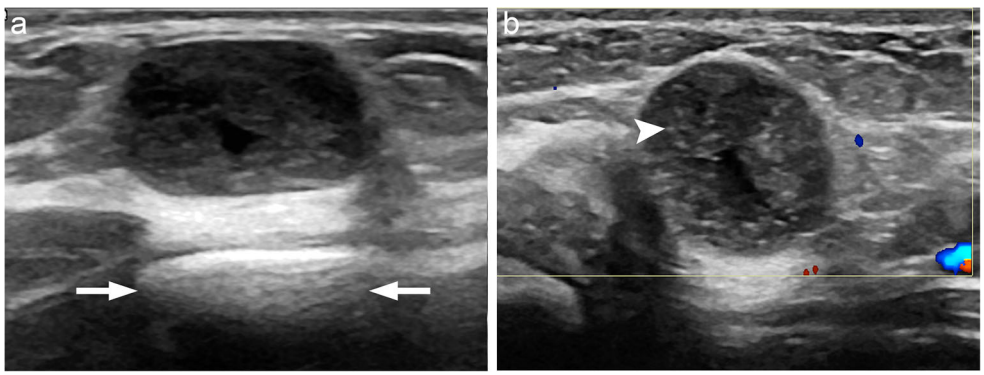

Fig. 23 Dermoid cyst in a 23-month-old girl presenting with a painless lump on her chest for 1 week. **a, b** Longitudinal gray-scale (**a**) and transverse color Doppler (**b**) US images show a well-defined avascular subcutaneous lesion with posterior acoustic enhancement (*arrows*), edge shadowing, and scattered internal echogenic foci (*arrowhead*)

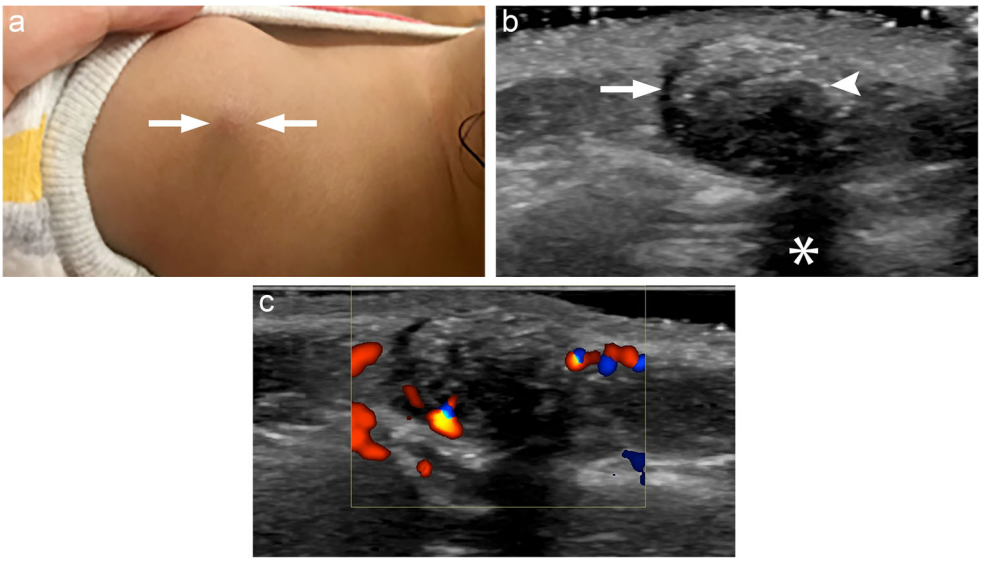

Fig. 24 Pilomatricoma in an 11-month-old girl presenting with painless lump for 2 months. **a** Clinical photograph shows a pebble-like mass with bluish discoloration (*arrows*). **b** Longitudinal gray-scale US image shows a well-circumscribed heterogeneous subcutaneous mass with a hypoechoic rim (*arrow*), internal echogenic foci (*arrowhead*) and shadowing (*asterisk*). **c** Color Doppler US image demonstrates peripheral vascularity with only minimal flow centrally

sinus tract extending to the skin. Like other cysts, these lesions are avascular. If there is surrounding hyperemia, then chemical inflammation from rupture is much more likely than true infection, especially in the setting of mural irregularity.

Pilomatricoma

Pilomatricoma is a relatively common benign tumor arising from the hair cortex cells. It is usually asymptomatic and presents as a small, slow-growing, mobile, pebble-like mass. The overlying skin often has a bluish discoloration but can become inflamed and even ulcerate later in presentation. These lesions are usually solitary and, though the most common location is the head and neck, approximately 8% arise in the trunk [76]. Spontaneous regression has never been reported, malignant transformation has been rarely described, and incomplete excision almost always results in recurrence. Therefore, the recommended treatment is complete excision, which results in an estimated recurrence rate of 1.4% [76]. The accuracy of clinical diagnosis, however, has been reported as low as 16% [76].

The sonographic characteristics of pilomatricoma have been well described [77–80]. The lesion is typically rounded and well-circumscribed, with a hypoechoic rim (Fig. 24). The echotexture is heterogeneous, most commonly with reticulation or scattered echogenic foci from calcifications. The overall echogenicity is most commonly hypoechoic but can be iso- or even hyperechoic. Dense calcifications often result in shadowing, but posterior acoustic enhancement can also be seen. Color Doppler demonstrates both internal and peripheral vascularity, more pronounced along the periphery. It has recently been proposed that hypoechogenicity, heterogeneous echotexture, scattered calcifications and hypoechoic rim are the sonographic characteristics that yield the highest diagnostic accuracy [79].

Conclusion

A palpable chest wall mass is a very common pediatric clinical concern. When imaging is requested, US is usually the ideal modality for the initial radiologic evaluation because there is no ionizing radiation or need for sedation. A thorough knowledge of the sonographic appearances of benign masses can help improve diagnostic confidence, minimize the need for additional imaging, and avoid biopsy or excision when appropriate.

Declarations

Conflicts of interest None

References

1. Donnelly LF, Taylor CN, Emery KH, Brody AS (1997) Asymptomatic, palpable, anterior chest wall lesions in children: is cross-sectional imaging necessary? Radiology 202:829–831
2. DiPietro M, Leschied J (2017) Pediatric musculoskeletal ultrasound. Pediatr Radiol 47:1144–1154
3. Mong A, Epelman M, Darge K (2012) Ultrasound of the pediatric chest. Pediatr Radiol 42:1287–1297
4. Restrepo R, Lee EY (2012) Updates on imaging of chest wall lesions in pediatric patients. Semin Roentgenol 47:79–89
5. Supakul N, Karmazyn B (2013) Ultrasound of the pediatric chest — the ins and outs. Semin Ultrasound CT MR 34:274–285
6. Kim HW, Yoo SY, Oh S et al (2020) Ultrasonography of pediatric superficial soft tissue tumors and tumor-like lesions. Korean J Radiol 21:341–355
7. Navarro OM (2009) Imaging of benign pediatric soft tissue tumors. Semin Musculoskelet Radiol 13:196–209
8. Navarro OM (2020) Pearls and pitfalls in the imaging of soft-tissue masses in children. Semin Ultrasound CT MR 41:498–512
9. García-Peña P, Barber I (2010) Pathology of the thoracic wall: congenital and acquired. Pediatr Radiol 40:859–868

10. Wong K, Hung IJ, Wang CR, Lien R (2004) Thoracic wall lesions in children. Pediatr Pulmonol 37:257–263
11. Donnelly LF, Frush DP, Foss JN et al (1999) Anterior chest wall: frequency of anatomic variations in children. Radiology 212:837–840
12. Supakul N, Karmazyn B (2013) Ultrasound evaluation of costochondral abnormalities in children presenting with anterior chest wall mass. Semin Ultrasound CT MR 201:W336–W341
13. Snosek M, Tubbs RS, Loukas M (2014) Sternalis muscle, what every anatomist and clinician should know. Clin Anat 27:866–884
14. Romanini MV, Calevo MG, Puliti A et al (2018) Poland syndrome: a proposed classification system and perspectives on diagnosis and treatment. Semin Pediatr Surg 27:189–199
15. Talbot BS, Gange CP Jr, Chaturvedi A et al (2017) Traumatic rib injury: patterns, imaging pitfalls, complications, and treatment. Radiographics 37:628–651
16. Griffith JF, Rainer TH, Ching AS et al (1999) Sonography compared with radiography in revealing acute rib fracture. AJR Am J Roentgenol 173:1603–1609
17. Smeets A, Robben S, Meradji M (1990) Sonographically detected costo-chondral dislocation in an abused child — a new sonographic sign to the radiological spectrum of child abuse. Pediatr Radiol 20:566–567
18. Kelloff J, Hulett R, Spivey M (2008) Acute rib fracture diagnosis in an infant by US: a matter of child protection. Pediatr Radiol 39:70–72
19. Orth RC, Laor T (2009) Isolated costal cartilage fracture: an unusual cause of an anterior chest mass in a toddler. Pediatr Radiol 39:985–987
20. Malghem J, Vande Berg BC, Lecouvet FE, Maldague BE (2001) Costal cartilage fractures as revealed on CT and sonography. AJR Am J Roentgenol 176:429–432
21. Douis H, Saifuddin A (2012) The imaging of cartilaginous bone tumours. I. Benign lesions. Skelet Radiol 41:1195–1212
22. Richardson RR (2005) Variants of exostosis of the bone in children. Semin Roentgenol 40:380–390
23. Murphey MD, Choi JJ, Kransdorf MJ et al (2000) Imaging of osteochondroma: variants and complications with radiologic-pathologic correlation. Radiographics 20:1407–1434
24. Bernard SA, Murphey MD, Flemming DJ, Kransdorf MJ (2010) Improved differentiation of benign osteochondromas from secondary chondrosarcomas with standardized measurement of cartilage cap at CT and MR imaging. Radiology 255:857–865
25. Petscavage-Thomas JM, Walker EA, Logie CI et al (2014) Soft-tissue myxomatous lesions: review of salient imaging features with pathologic comparison. Radiographics 34:964–980
26. Giard M, Pineda C (2014) Ganglion cyst versus synovial cyst? Ultrasound characteristics through a review of the literature. Rheumatol Int 35:597–605
27. Teefey SA, Dahiya N, Middleton WD et al (2008) Ganglia of the hand and wrist: a sonographic analysis. AJR Am J Roentgenol 191:716–720
28. Murphey MD, Carroll JF, Flemming DJ et al (2004) From the archives of the AFIP: benign musculoskeletal lipomatous lesions. Radiographics 24:1433–1466
29. Sheybani EF, Eutsler EP, Navarro OM (2016) Fat-containing soft-tissue masses in children. Pediatr Radiol 46:1760–1773
30. Murphey MD, Ruble CM, Tyszko SM et al (2009) From the archives of the AFIP: musculoskeletal fibromatoses: radiologic-pathologic correlation. Radiographics 29:2143–2173
31. Bang M, Kang BS, Hwang JC et al (2012) Ultrasonographic analysis of subcutaneous angiolipoma. Skelet Radiol 41:1055–1059
32. DeFilippis EM, Arleo EK (2014) The ABCs of accessory breast tissue: basic information every radiologist should know. AJR Am J Roentgenol 202:1157–1162
33. Weinstein SP, Conant EF, Orel SG et al (2000) Spectrum of US findings in pediatric and adolescent patients with palpable breast masses. Radiographics 20:1613–1621
34. Chung EM, Cube R, Hall GJ et al (2009) From the archives of the AFIP: breast masses in children and adolescents: radiologic-pathologic correlation. Radiographics 29:907–931
35. Dickson G (2012) Gynecomastia. Am Fam Physician 85:716–722
36. Valeur N, Rahbar H, Chapman T (2015) Ultrasound of pediatric breast masses: what to do with lumps and bumps. Pediatr Radiol 45:1584–1599
37. Appelbaum AH, Evans GF, Levy KR et al (1999) Mammographic appearances of male breast disease. Radiographics 19:559–568
38. Moon S, Lim HS, Ki SY (2019) Ultrasound findings of mammary duct ectasia causing bloody nipple discharge in infancy and childhood. J Ultrasound Med 38:2793–2798
39. McHoney M, Munro F, MacKinlay G (2011) Mammary duct ectasia in children: report of a short series and review of the literature. Early Hum Dev 87:527–530
40. Stevens DL, Bisno AL, Chambers HF et al (2014) Practice guidelines for the diagnosis and management of skin and soft tissue infections: 2014 update by the Infectious Diseases Society of America. Clin Infect Dis 59:e10
41. Pulia M, Calderone M, Meister J et al (2014) Update on management of skin and soft tissue infections in the emergency department. Curr Infect Dis Rep 16:1–9
42. Fenster DB, Renny MH, Ng C, Roskind CG (2015) Scratching the surface: a review of skin and soft tissue infections in children. Curr Opin Pediatr 27:303–307
43. Chao HC, Lin SJ, Huang YC, Lin TY (2000) Sonographic evaluation of cellulitis in children. J Ultrasound Med 19:743–749
44. Nelson C, Chen A, Bellah R et al (2018) Ultrasound features of purulent skin and soft tissue infection without abscess. Emerg Radiol 25:505–511
45. Crone AM, Wanner MR, Cooper ML et al (2020) Osteomyelitis of the ribs in children: a rare and potentially challenging diagnosis. Pediatr Radiol 50:68–74
46. Bureau NJ, Chhem RK, Cardinal E (1999) Musculoskeletal infections: US manifestations. Radiographics 19:1585–1592
47. Shyy W, Knight RS, Goldstein R et al (2016) Sonographic findings in necrotizing fasciitis: two ends of the spectrum. J Ultrasound Med 35:2273–2277
48. Campbell EA, Wilbert CD (2021) Foreign body imaging. In: StatPearls. StatPearls Publishing, Treasure Island
49. Moreira BL, Marchiori E (2020) Self-limiting sternal tumor of childhood: a “do not touch” lesion. J Pediatr 221:260–261
50. te Winkel ML, Lequin MH, de Bruyn JR et al (2010) Self-limiting sternal tumors of childhood (SELSTOC). Pediatr Blood Cancer 55:81–84
51. Ilivitzki A, Sweed Y, Beck N, Militianu D (2013) Sternal pseudotumor of childhood: don't touch the lesion. J Ultrasound Med 32:2199–2203
52. Fletcher CDM (2014) The evolving classification of soft tissue tumours — an update based on the new 2013 WHO classification. Histopathology 64:2–11
53. Goldblum JR, Folpe AL, Weiss SW (2020) Perivascular tumors. In: Enzinger and Weiss's soft tissue tumors, 7th edn. Elsevier, Philadelphia
54. Robbin MR, Murphey MD, Temple HT et al (2001) Imaging of musculoskeletal fibromatosis. Radiographics 21:585–600
55. Koujok K, Ruiz R, Hernandez R (2005) Myofibromatosis: imaging characteristics. Pediatr Radiol 35:374–380
56. Sargar KM, Sheybani EF, Shenoy A et al (2016) Pediatric fibroblastic and myofibroblastic tumors: a pictorial review. Radiographics 36:1195–1214
57. Ji Y, Hu P, Zhang C et al (2019) Fibrous hamartoma of infancy: radiologic features and literature review. BMC Musculoskelet Disord 20:356

58. Goldblum JR, Folpe AL, Weiss SW (2020) Fibrous tumors of infancy and childhood. In: Enzinger and Weiss's soft tissue tumors, 7th edn. Elsevier, Philadelphia
59. Lee S, Choi Y, Cheon J et al (2014) Ultrasonographic features of fibrous hamartoma of infancy. Skelet Radiol 43:649–653
60. Seguier-Lipszyc E, Hermann G, Kaplinski C, Lotan G (2011) Fibrous hamartoma of infancy. J Pediatr Surg 46:753–755
61. Mulligan PR, Prajapati HJS, Martin LG, Patel TH (2014) Vascular anomalies: classification, imaging characteristics and implications for interventional radiology treatment approaches. Br J Radiol 87: 20130392
62. Merrow AC, Gupta A, Patel MN, Adams DM (2016) 2014 revised classification of vascular lesions from the International Society for the Study of Vascular Anomalies: radiologic-pathologic update. Radiographics 36:1494–1516
63. Behr GG, Johnson C (2013) Vascular anomalies: hemangiomas and beyond — part 1, fast-flow lesions. AJR Am J Roentgenol 200: 414–422
64. Flors L, Leiva-Salinas C, Maged IM et al (2011) MR imaging of soft-tissue vascular malformations: diagnosis, classification, and therapy follow-up. Radiographics 31:1321–1340
65. Olivieri B, White CL, Restrepo R et al (2016) Low-flow vascular malformation pitfalls: from clinical examination to practical imaging evaluation — part 2, venous malformation mimickers. AJR Am J Roentgenol 206:952–962
66. Trop I, Dubois J, Guibaud L et al (1999) Soft-tissue venous malformations in pediatric and young adult patients: diagnosis with Doppler US. Radiology 212:841–845
67. Behr GG, Johnson CM (2013) Vascular anomalies: hemangiomas and beyond — part 2, slow-flow lesions. AJR Am J Roentgenol 200:423–436
68. Beggs I (1997) Pictorial review: imaging of peripheral nerve tumours. Clin Radiol 52:8–17
69. Patel NB, Stacy GS (2012) Musculoskeletal manifestations of neurofibromatosis type 1. AJR Am J Roentgenol 199:W99–W106
70. Gruber H, Glodny B, Bendix N et al (2007) High-resolution ultrasound of peripheral neurogenic tumors. Eur Radiol 17:2880–2888
71. Pavlus JD, Carter BW, Tolley MD et al (2016) Imaging of thoracic neurogenic tumors. AJR Am J Roentgenol 207:552–561
72. Koeller KK, Alamo L, Adair CF, Smirniotopoulos JG (1999) Congenital cystic masses of the neck: radiologic-pathologic correlation. Radiographics 19:121–123
73. Vittore CP, Goldberg KN, McClatchey KD, Hotaling AJ (1998) Cystic mass at the suprasternal notch of a newborn: congenital suprasternal dermoid cyst. Pediatr Radiol 28:984–986
74. Bansal AG, Oudsema R, Masseaux JA, Rosenberg HK (2018) US of pediatric superficial masses of the head and neck. Radiographics 38:1239–1263
75. Kim H, Kim S, Lee S et al (2011) Subcutaneous epidermal inclusion cysts: ultrasound (US) and MR imaging findings. Skelet Radiol 40:1415–1419
76. Jones CD, Ho W, Robertson BF et al (2018) Pilomatrixoma: a comprehensive review of the literature. Am J Dermatopathol 40: 631–641
77. Lim H, Im S, Lim G et al (2007) Pilomatricomas in children: imaging characteristics with pathologic correlation. Pediatr Radiol 37: 549–555
78. Hwang JY, Lee SW, Lee SM (2005) The common ultrasonographic features of pilomatricoma. J Ultrasound Med 24:1397–1402
79. Choo H, Lee S, Lee Y et al (2010) Pilomatricomas: the diagnostic value of ultrasound. Skelet Radiol 39:243–250
80. Bulman JC, Ulualp SO, Rajaram V, Koral K (2016) Pilomatricoma of childhood: a common pathologic diagnosis yet a rare radiologic one. AJR Am J Roentgenol 206:182–188